RSC Advances

ROYAL SOCIETY OF CHEMISTRY

www.rsc.org/advances

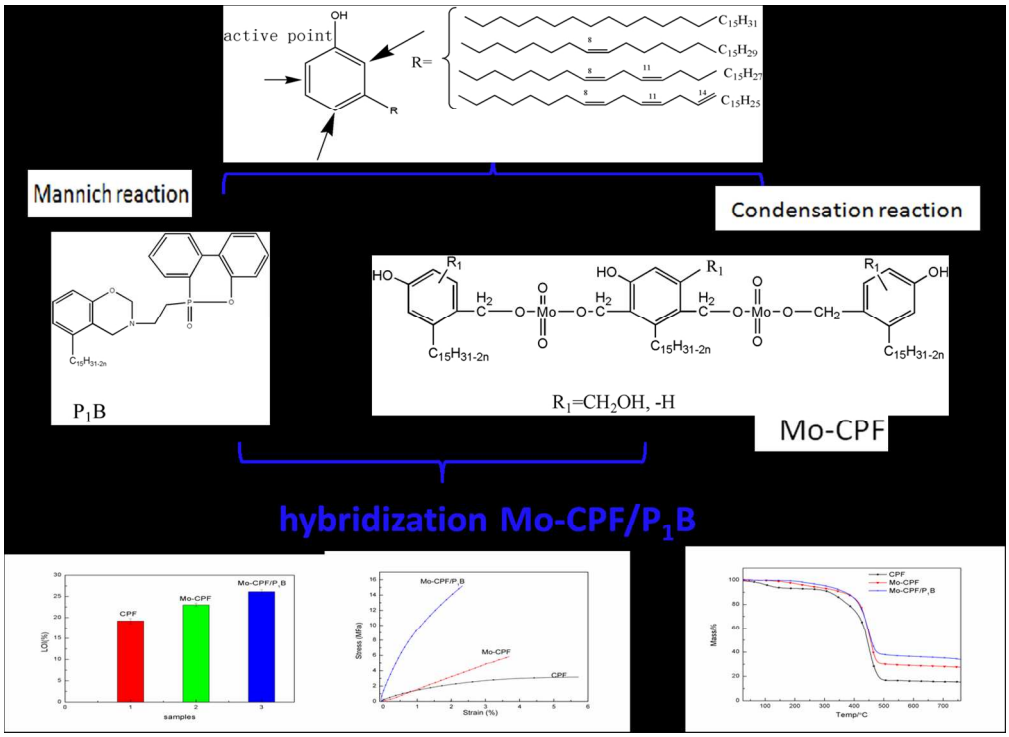

254x184mm (150 x 150 DPI)

Journal Name

ARTICLE

Fabrication and Property of Hybrid Mo-CPF/P_1B from cardanol

Guomei Xu [a, b],Tiejun Shi[a],Yu Xiang [a] ,Wei Yuan[a] and Quan Wang[a]

Received 27th May 2015,
Accepted 00th January 2015

DOI: 10.1039/x0xx00000x

www.rsc.org/

Abstract: Mo-CPF/P_1B hybrid has been prepared from molybdenum modified cardanol phenolic (Mo-CPF) and cardanol benzoxazine with phosphorus (P_1B). Cardanol benzoxazine with phosphorus (P_1B) has been synthesized from cardanol-allylamine-based benzoxazine (BZc-a) and DOPO (9, 10-dihydro-9-oxa-10-phosphaphenanthrene-10-oxide). Cardanol phenolic modified with molybdenum (Mo-CPF) has been synthesized by reacting cardanol-based phenolic resins (CPF) with ammonium molybdate tetrahydrate at 150 ℃, where the CPF was synthesized from cardanol and paraformaldehyde in presence of sodium hydroxide at 65 ℃. The synthesized CPF and Mo-CPF were characterized by ^{1}H-NMR and size exclusion chromatography (SEC). Mixed Mo-CPF with P_1B, cured the mixtures at 110 ℃ for 4 hrs and got Mo-CPF/P_1B hybrid. The property of Mo-CPF/P_1B hybrid was investigated; the results demonstrated that mechanical and thermal properties, together with flame retardance were greatly improved. Dynamic Mechanical Analysis (DMA) measurements results indicated that CPF, Mo-CPF and Mo-CPF/P_1B could all sustain a large amount of stress and the elongations at break were different. DMA measurements suggested that Tg of CPF, Mo-CPF and Mo-CPF/P_1B were 98 ℃, 170 ℃ and 131 ℃ respectively. Mo-CPF/P_1B exhibited better flame retardance after conjugating with molybdenum and phosphorus. TGA results suggested Mo-CPF/P_1B exhibited better thermal properties. Field emission electron microscope (FE-SEM) suggested that molybdenum were randomly distributed in Mo-CPF and Mo-CPF/P_1B, and EDX indicated that molybdenum and phosphorus were randomly distributed in the Mo-CPF/P_1B.

Key words: cardanol-based phenolic resins; molybdenum; DOPO; mechanics; flame retardance

1. INTRODUCTION

Phenolic resin (PF) was prepared firstly by A. von Baeyer as early as 1872; however, it attracts technical and commercial interests till to 1907, which was attributed to Leo H. Baekeland [1]. Since then it play an important role during the process of social development and own century-long history. Nowadays, PF still be very popular and attracts much attention both in experimental and theoretical scientific fields due to its significant advantages [2], such as thermal stability, adhesive property and so on. In addition, PF properties can be improved by combined with reinforcing and filling ingredients. For example, Chun-Te Lin et al reported preparation of molybdenum/phenolic resin by blending m-AIN with molybdenum/phenolic resin [3], the mechanical properties of the composite were drastically improved which could be applied as a binder for diamond cutting wheels.

Benzoxazine could be normally synthesized from phenol, formaldehyde and primary amine [4]. During the synthesis, ring-opening polymerization would form a novel phenolic structure in presence of catalysts or under heating [5]. Lin Jin et al [6] have reported a bis(benzoxazine-maleimide)s was synthesized with hydroxyphenylmaleimide, paraformaldehyde and various diamines. 4-cyanophenol [7] was used to synthesis benzoxazine monomer via Mannich reaction. These materials are all petroleum-based. Long-

[a] School of Chemistry and Chemical Engineering of Hefei University of Technology, Hefei, 230009, People's Republic of China
[b] School o f Materials and Chemical Engineering of West Anhui University, Anhui, Lu'an, 237012, People's Republic of China

term use of petroleum-based materials not only constitutes a threat to human health but also aggravate the crises of petroleum. So, considering sustainable development and ecological issues, it is vital to look for and use eco-friendly alternatives, and various alternatives have also been explored in production of benzoxazine. A typical example is cardanol which is bio-based and require no consumption of petroleum [8]. Cardanol can be obtained from costless and sustainable cashew nut shell liquid [9], which is a mixture of non-isoprenoic phenols [10] and also contains a *meta*-substituted long unsaturated alkyl chain [11]. Emanuela Calo` et al [12] prepared a novel benzoxazine pre-polymer deriving from cardanol. Various products have also been prepared from cardanol such as phenolic resin [13], cross-linked polymer [14], and so on [15].

Herein, we propose to prepare a hybrid cardanol-typed [16] material through reacting PF with benzoxazine, aiming to improve the fragility of benzoxazine by PF (Scheme 1). In addition, ammonium molybdate tetrahydrate was used to modify PF to improve the crosslinking of PF (Scheme 2). Liquid benzoxazine contained DOPO (9, 10-dihydro-9-oxa-10-phosphaphenanthrene-10-oxide) is used as to endow the hybrid with good flame retardance [17]. Mechanics, flame retardances and thermal properties of the hybrid materials will be investigated.

Scheme.1 synthesis route of P_1B

Scheme.2 synthesis route of CPF and Mo-CPF

2. EXPERIMENTAL

2.1 Materials

Cardanol is obtained from Shangdong Haobo Biological Material Co., Ltd. M=304.52; DOPO, and paraformaldehyde is purchased from Shanghai Chemical Reagents Company and used as received; Hexaammonium molybdate tetrahydrate was obtained from Anhui Kehua Fine Chemical Industry Research Institute.

A liquid benzoxazine contained DOPO (P_1B) was self-prepared; 23 g BZc-a react with 2.8 g DOPO in 200mL alcohol solution. The reaction continued for 8 hrs at 65℃ under refluxing in nitrogen atmosphere, and then stopped reacting and removed alcohol under vacuum; a maroon sticky liquid product was isolated. The chemical structure of P_1B was shown in Scheme 1 and the other properties were present in elsewhere [18]. All other chemicals are used as received.

2.2 Preparation of cardanol-based phenolic resins (CPF)

Typically, 258 g cardanol was placed in a 500 mL three-neck round flask equipped with a mechanical stirrer, thermometer and refluxing condenser. Upon heating up to 65℃ gradually, 32 g of paraformaldehyde was added slowly into the reaction mixture, in presence of 2 g NaOH. Reaction was conducted under refluxing for six hrs when the solution was very viscous. The synthetic route was shown in Scheme 2. Finally, maroon sticky product was obtained [14].

2.3 Modification of cardanol-based phenolic resin with molybdenum (Mo-CPF)

The preparation process of Mo-CPF is similar to the synthesis of CPF. Typically, into a three-neck round flask reactor, 100 g CPF and 10 g hexaammonium molybdate tetrahydrate were added and stirred at 150 ℃ for 4 hrs. The reaction was stopped and mixture was washed with water to remove the impurities and side products. Finally, brown liquid was obtained as product (Scheme 2).

2.4 Preparation of Mo-CPF/P_1B hybrid material

Mo-CPF/P_1B was prepared by solution blending. Typically, 20 g Mo-CPF was mixed with 20 g P_1B in alcohol at elevated temperature. Then the mixture was heated up to 80 ℃ and reacted for 2 hrs before final product could be obtained, ultrasonication was applied to promote the blending rate.

Then the blending was heated in a stainless rectangular mold in an air-circulating oven for curing, and then continuing to cure at 110 ℃ for 4 hrs and got Mo-CPF/P_1B hybrid.

2.5. Measurements

^{1}H-NMR spectra were recorded in DMSO-d6 on a VNMRS600 instrument of 600MHz (Agilent, America). Size exclusion chromatography (SEC) was conducted on Waters 515 pump and Waters 2414 differential refractive index (RI) detector (set at 40 °C) using three linear Styragel HR1, HR2 and HR4 columns. Tetrahydrofuran (THF) was used as eluent and the flow rate is 0.3 mL/min. The number-average molecular weight (Mn) and polydispersity (Mw/Mn) data are reported relative to polystyrene standards. Field emission electron microscope (FE-SEM) and energy-dispersive X-ray spectrum (EDX) observations were

performed on a FEI Sirion SU8020 system with an energy-dispersive X-ray elemental composition analyzer at an accelerating voltage of 3 kV. Before measurements, the specimens were exposed in a vacuum oven and a thin layer of gold was sputter-sprayed on their surface. Dynamic mechanical analysis (DMA) was performed on a DMA Q800 instrument. The cured specimens (length 8.8 mm, width 4.8 mm and thickness 1.8 mm) were investigated in a tensile deformation mode from 35 to 300 ◦C at a heating rate of 5 K/min and also subject to multi-frequency- strain at room temperature. The burning behaviour by limited oxygen index was recorded according to GB/T 2406 standard with a test specimen bar of 90 mm in length, 7 mm in width and about 2.5 mm in thickness, which was conducted on a XZT-100A (ChengDe Testing Machine Co., Ltd, China) apparatus for Limited Oxygen Index Testing. Each compound was prepared with two test specimen. The flame retardant experiment was conducted by adjusting the proportion of nitrogen and oxygen in vertical glass bottle.

Thermogravimetric Analysis (TGA) was performed on NETZSCH STA 449F3 at a heating rate of 10 K/min up to 800 ℃ in nitrogen atmosphere. All cured specimen 5-8 mg were put in a platinum pan. The gas flow rate was at 50 mL/min.

3. Results and discussion

3.1 Synthesis and Characterizations

Mo-CPF/P_1B has been prepared by blending P_1B with Mo-CPF. The structure of CPF and Mo-CPF was confirmed by ^{1}HNMR [19] and SEC. EDX layered images indicated that molybdenum and phosphorus were randomly distributed in the Mo-CPF/P_1B. Details can be found in following. Table 1 listed the thermal properties of Mo-CPF/P_1B.

Table 1 Thermal property of CPF, Mo-CPF and Mo-CPF/P_1B

Fig.1 ^{1}H-NMR spectrum of CPF

Fig.2 ^{1}H-NMR spectrum of cardanol

CPF is a phenolic resin prepared from cardanol, Fig.1 and Fig.2 show the results of ^{1}H-NMR spectrum of CPF and cardanol, these spectrums were all performed in DMSO, the chemical shift of DMSO and water was setting as 2.46 ppm and 3.3 ppm, respectively. By comparing Fig.1 and Fig.2, it could be found that there were another three peaks appeared in the ^{1}H-NMR spectrum of CPF than that of cardanol. Firstly, a peak at 3.14 ppm, which corresponding to the proton in the CH_2 groups between two benzenes in CPF. Secondly, four peaks appeared among 4.3-4.6 ppm, these were the characteristic protons of active hydroxymethyl or methyl ether (-CH_2OH- or –CH_2OCH_2-), which showed benzene rings in CPF would be connected with methyl ether bridge or existed many active hydroxymethyl groups in CPF. CPF could soluble in ethanol, so this kind of phenolic resin from cardanol has low molecular weight. Peaks appeared at 3.14 and among 4.3-4.6 ppm would due to be many oligomers formed and a variety of substitute existed between benzene rings in CPF. Thirdly, the aromatic protons appeared as multiplet at 7.2, 7.1, 7.05 ppm, which also demonstrated that many kinds of substitute formed between benzene rings. The other characteristic protons of CPF were almost the same as the ^{1}H-NMR spectrum of cardanol. Except that one peak at 5.97 ppm, which disappeared and showed one aromatic proton in cardanol was reacted and be substituted [18]. All these data confirmed that CPF was successfully synthesized from cardanol [5].

Fig.3 ^{1}H-NMR spectrum of Mo-CPF

The ^{1}H-NMR spectrum of Mo-CPF is shown in Fig.3. Compared Fig.3 with Fig.1 and Fig.2, it could be found that three pronounced difference existed in Fig.3. Firstly, a peak at 3.14 ppm corresponding to the methylene bridge between benzene rings disappeared in the ^{1}H-NMR spectrum of Mo-CPF, which showed the methylene bridge broke after CPF modified by molybdenum, so there was no methylene bridge between benzene rings in Mo-CPF. Secondly, the peaks at 4.47-4.3 ppm corresponding to the characteristic protons of active hydroxymethyl or methyl ether (-CH_2OH- or –CH_2OCH_2-) also appeared in Fig.3, however, the intensity and quantity of peaks all decreased, which confirmed that -Mo-O-CH_2- group generated between benzene rings after CPF modified by molybdenum. Thirdly, a peak at 9.15 ppm appeared, which would be the characteristic protons of active phenolic protons of –OH, which not be found in the ^{1}H-NMR spectrum of CPF.

Fig.4 SEC chromatograms of CPF

Fig.5 SEC chromatograms of Mo-CPF

The SEC chromatograms of CPF and Mo-CPF are present in Fig.4-5, which both indicate the formation of broad dispersed polymer. However, Fig.4 exhibit that the molecular distribution of CPF is too broad to predict the molecular weight, oligomers effluent

about 27 minute, then the monomer of CPF effluent after 30 minute. Fig.5 show the part of molecular distribution of Mo-CPF could be calculated and the values of number-average molecular weight (Mn), weight-average molecular weight (Mw) and molecular weight distribution (MWD=Mw/Mn) of the Mo-CPF are given in Table 2. Long chain alkyd resins exhibit in general low Mn, Mw, and Mw/Mn. According to all these data, the structure of CPF and Mo-CPF was given in scheme 2.

Table 2 Molecular weight and molecular weights distribution of Mo-CPF

In order to confirm the element distributed on the surface was changed, energy-dispersive X-ray spectrum (EDX) of Mo-CPF and Mo-CPF/P_1B was examined and the result is shown in Fig.6-7 [3]. The images display that there are carbon, oxygen and molybdenum elements exist on the surface of Mo-CPF, and the green spots on the top of Fig.6 are molybdenum element which distributes uniformly in the Mo-CPF. At the bottom of Fig.6 is the mapping of each element, the mapping of carbon element is referred as a controlled image. Comparing the mapping of molybdenum element with that of carbon, it is could be seen the molybdenum is dispersed in CPF matrix uniformly and exhibits a tougher surface.

The energy-dispersive X-ray spectrum (EDX) of Mo-CPF/P_1B is shown in Fig.7. By comparing the images display not only carbon, oxygen and molybdenum elements exist on the surface of Mo-CPF/P_1B, but also phosphorus element exist in Mo-CPF/P_1B. At the bottom of Fig.7 is the mapping of each element, the mapping of carbon element is referred as a controlled image. It could be found that the molybdenum and phosphorus is dispersed in composite uniformly. The irregular granules are molybdenum element.

Fig. 6 EDX layered spectrum of Mo-CPF

Fig. 7 EDX layered spectrum of Mo-CPF/P_1B

Field emission electron microscope (FE-SEM) was applied to study the surface morphologies of cured CPF, Mo-CPF and Mo-CPF/P_1B, and typical images are shown in Fig.8-10. Compared with the relatively smooth surface of CPF and Mo-CPF, the surface of Mo-CPF/P_1B is much more complicated. CPF showed relatively smooth glassy fracture surface with cracks in different cross-sections, and this suggested phenolic resin is brittle [20].

Fig.8 FESEM photographs of fracture surface of CPF

Fig. 9 FESEM photographs of fracture surface of Mo-CPF

Fig. 10 FESEM photographs of fracture surface of Mo-CPF/P_1B

Cured Mo-CPF showed many spherical-like protrusions on the surface (Fig.9) and these particles maybe molybdenum particles [21]. The surface was tougher than CPF, suggesting the successful modification of hexaammonium molybdate tetrahydrate. The surface of Mo-CPF/P_1B was much more complicated: more wrinkles and particles appeared. The compatibility between Mo and P with CPF was very good after the copolymerization, as no phase separation happened (refer to high magnification image (Fig.10b)). It seemed that similar alkyl chain of Mo-CPF and P_1B contributed to the improvement of compatibility of final product.

3.2 Properties study

3.2.1 Mechanical Properties of Mo-CPF/P_1B

Dynamic mechanical analysis (DMA) is used to measure the elastic behavior especially the viscoelastic properties of polymer materials [22]. In our study, the measurements were performed by multifrequency strain test at a heating rate of 5 K/min from 30 ℃ to 300 ℃. The results are shown in Fig.11, which indicated that there is only one α relaxation phenomena during the glass transition. Each tan δ curve of cured CPF, Mo-CPF and Mo-CPF/P_1B films has one peak centered at about 98, 170 and 131 ℃, respectively. The cured Mo-CPF and Mo-CPF/P_1B showed a drastic increase in the Tg than neat CPF, which might be due to the incorporation of molybdenum resulting in formation of a new network linked by –Mo-O bonds [23]. When introducing phosphorus into Mo-CPF/P_1B, the incorporation of P_1B decrease the density of link –Mo-O group, resulted in the decrease of Tg [24].

Our measurements indicated that cured CPF resin had a broad Tg transition area ranging from 98℃ to 200℃, which may due to the complicated structures formed after the condensation between functional groups such as CH_2OH or -OH in CPF. However, cured Mo-CPF/P_1B resin showed a step change of tan δ curve after the temperature increased to 200℃. As glass transition is normally affected by the molecular mobility of materials cooperative units, in our system, the frequency of the cooperative rearrangement of co-

polymerized Mo-CPF and P_1B could be correspond to the measurement frequency, resulting in a step. The present results indicated that Tg could be manipulated to high temperature by introducing molybdenum in CPF [25].

The cured specimens (length 17.5 mm, width 10.5 mm and thickness 3.92 mm) were investigated with DMA Controlled Force in a Single Cantilever mode at a heating rate of 5 K/min at room temperature. The stress-strain curves of CPF, Mo-CPF and Mo-CPF/P_1B are plotted in Fig.12. The bottom curve with dot signs is the stress-strain curve for cured CPF, is a typical stress-strain curve for a phenolic resin and the curve is similar to linear. The middle curve with dot signs is the stress-strain curve for cured Mo-CPF. The top curve with triangle signs is the stress-strain curve for cured Mo-CPF/P1B. As shown in Fig.12, all resins exhibited a plastic behaviour. As comparison, Mo-CPF/P_1B showed the best mechanical properties, highest flexural modulus with 1019 MPa compared to the others (123.7 MPa for CPF and 167.7 MPa for Mo-CPF), which may be donated by the lightly-crosslinking network formed after conjugating CPF with Mo and P. Therefore the mechanics properties could be raised by treating with molybdenum and phosphorus [26].

Fig. 11 DMA curves of cured CPF, Mo-CPF and Mo-CPF/P_1B

Fig.12 stress–strain curves of cured CPF, Mo-CPF and Mo-CPF/P_1B

3.2.2 Flame retardancy of cured CPF, Mo-CPF and Mo-CPF/P_1B

DOPO materials normally have efficient flame inhibition, because DOPO could release PO in process of pyrolysis [27]. Here, we measured the fire retardancy of different materials according to Chinese standard of GB/T 2406. As shown in Fig.13, the limited oxygen index (LOI) of Mo-CPF/P1B (26.1) is highest compared to CPF (19.2) and Mo-CPF (23.0). CPF is a typical flammable material. The fire retardancy of Mo-CPF was better than CPF, as the conjugation of Mo could crosslinked the CPF which blocked the heat transfer and helped to improve the fire retardancy. Due to contribution from both of P_1B and crosslinked network of CPF after conjugation with Mo and P, LOI of Mo-CPF/P_1B reached 26.1, and this suggested the material to be almost non-flammable [7].

Fig.13 the burning behavior by limited oxygen index of cured CPF, Mo-CPF and Mo-CPF/P_1B

3.2.3 Thermal properties of cured CPF, Mo-CPF and Mo-CPF/P_1B

We also measured the thermal properties of the three materials using TGA and the results are shown in Fig.14. The total weight loss of Mo-CPF/P_1B was minimum (66%) compared to CPF and Mo-CPF, which suggested the best thermal stability among the three materials.

The bottom curve was the thermogravimetric curve of CPF, which showed two mass loss steps. The main decomposition stage happened at 300-500°C, and there was around 15% mass residual finally. After the reaction between hexaammonium molybdate tetrahydrate and CPF, which linked CPF polymer chain through -Mo-O- bonds, Mo-CPF showed better thermal stability: 27% mass residual finally. The main loss of Mo-CPF/P1B happened at temperature range of 400 °C to 482 °C and 34% mass residue was observed finally with significant difference from CPF and Mo-CPF. Significant differences in mass residue suggested that incorporate a little amount of molybdenum and phosphorus into Mo-CPF/P1B, which not only formed a structure linked with a lot of -Mo-O- and -O- groups between composites, and also P1B could release for phosphorus then worked in the gas phase and blocked the rate of decomposition. So the thermal stability of Mo-CPF/P1B was further improved. Details can be found in Table 1.

Fig.14 TGA curves of CPF, Mo-CPF and Mo-CPF/P_1B

4. Conclusions

Mo-CPF/P_1B hybrid with raw materials prepared from cardanol has been synthesized successfully. SEM images suggested that the surface of hybrid was much tougher than CPF and Mo-CPF. DMA, flame retardancy and TGA measurements all revealed that Mo-CPF/P_1B hybrid exhibit improved mechanical properties, perfect performance of flame retardance and good thermal stability,which confirming Mo-CPF and P_1B took recaction and formed a crosslinked structures during hybridizing. DMA study indicated the Tg of the hybrid is 131℃ which is different from CPF and Mo-CPF, the flexural modulus is 1019 Mpa. The flame-retardant property is also perfect and LOI value could reach 26.1. It had better thermal stability in air and 34% char yield at 800 °C.

Acknowledgement

Authors acknowledge the support from the National Natural Science Foundation of China (grant no.51273054); Authors also thanks the kindly help from Science and Technology Project of Anhui Province (grant no 1206c0805031 and 1406c085021); China and Engineering Technology Center of Fine Chemicals Engineering of AnHui, China; Authors also thanks the kindly help from professor Tao He of Hefei University of Technology.

References

1. Kopf PW, Little AD: **Phenolic Resins in ECT (online)**. In: *Kirk-Othmer Encyclopedia of Chemical Technology.* Edited by. Copyright John Wiley & Sons, Inc; 2000.
2. Rivero G, Villanueva S, Manfredi LB: *Fire and Materials* **2014**, (6):683-694.
3. Lin C-T, Lee H-T, Chen J-K: *Applied Surface Science* **2013**:297-307.
4. Lochab B, Varma IK, Bijwe J: *Journal of Thermal Analysis and Calorimetry* **2012**, (2):1357-1364.
5. Periyasamy T, Asrafali S, Muthusamy S: *New Journal of Chemistry* **2014**.
6. Jin L, Agag T, Ishida H: *European Polymer Journal* **2010**, (2):354-363.
7. Wang D, Li B, Zhang Y, Lu Z: *Journal of Applied Polymer Science* **2013**:516-522.
8. Lochab B, Varma IK, Bijwe J: *Journal of Thermal Analysis and Calorimetry* **2011**, (2):661-668.
9. Balgude D, Sabnis AS: *Journal of Coatings Technology and Research* **2013**, (2):169-183.
10. Voirin C, Caillol S, Sadavarte NV, Tawade BV, Boutevin B, Wadgaonkar PP: *Polymer Chemistry* **2014**, (9):3142-3162.
11. Balachandran VS, Jadhav SR, Vemula PK, John G: *Chemical Society Reviews* **2013**, (2):427-438.
12. Cal E, Maffezzoli A, Mele G, Martina F, Mazzetto SE, Tarzia A, Stifani C: *Green Chemistry* **2007**, (7):754.
13. Shukla SK, Maithani A, Srivastava D: *International Journal of Chemical Kinetics* **2013**, (7):469-476.
14. Bai W, Xiao X, Chen Q, Xu Y, Zheng S, Lin J: *Progress in Organic Coatings* **2012**, (3):184-189.
15. Vasapollo G, Mele G, Del Sole R: *Molecules* **2011**, (12):6871-6882.
16. Kathalewar M, Sabnis A: *Journal of Coatings Technology and Research* **2014**, (4):601-618.
17. Ma Y, Wang J, Xu Y, Wang C, Chu F: *Journal of Thermal Analysis and Calorimetry* **2013**, (3):1143-1151.
18. Xu G, Shi T, Wang Q, Liu J, Yi Y: *Journal of Applied Polymer Science* **2015**, (11):3534-3545.
19. Li C, Fan H, Wang D-Y, Hu J, Wan J, Li B: *Composites Science and Technology* **2013**:189-195.
20. Huang K, Zhang Y, Li M, Lian J, Yang X, Xia J: *Progress in Organic Coatings* **2012**, (1):240-247.
21. Zhao P, Zhou Q, Deng YY, Zhu RQ, Gu Y: *RSC advances* **2014**, (4):61634-41642.
22. Taheri-Behrooz F, Memar Maher B, Shokrieh MM: *Computational Materials Science* **2015**:411-415.
23. Bu Z, Hu J, Li B: *Thermochimica Acta* **2014**:244-253.
24. Zhang J, Zhu C, Geng P, Wei Y, Lu Z: *Journal of Applied Polymer Science* **2014**.
25. Chen Z, Chisholm BJ, Webster DC, Zhang Y, Patel S: *Progress in Organic Coatings* **2009**, (2):246-250.
26. Assanvo EF, Gogoi P, Dolui SK, Baruah SD: *Industrial Crops and Products* **2015**:293-302.
27. Yu H, Liu J, Wen X, Jiang Z, Wang Y, Wang L, Zheng J, Fu S, Tang T: *Polymer* **2011**, (21):4891-4898.

Lists of Figures Captions:

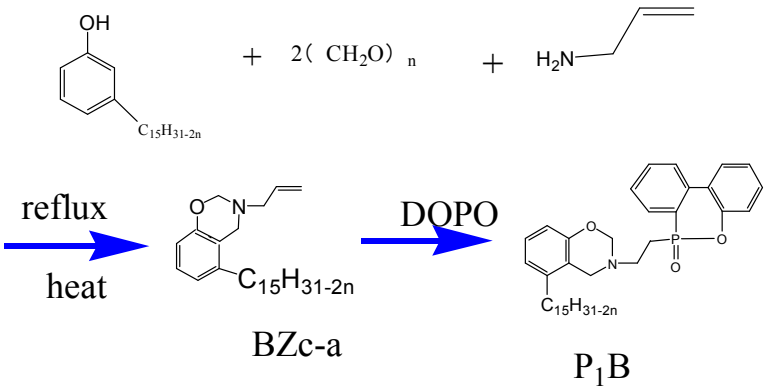

Scheme.1

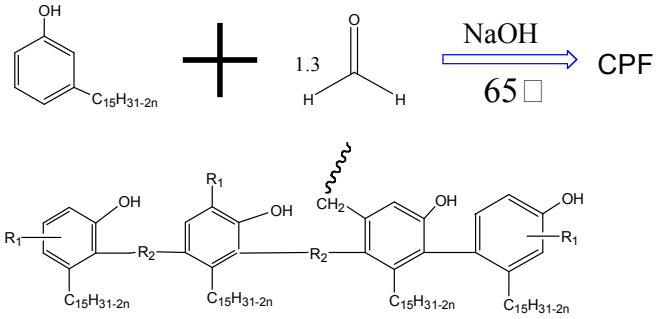

R_1=CH_2OH, -H; R_2=CH_2OCH_2-, -CH_2-

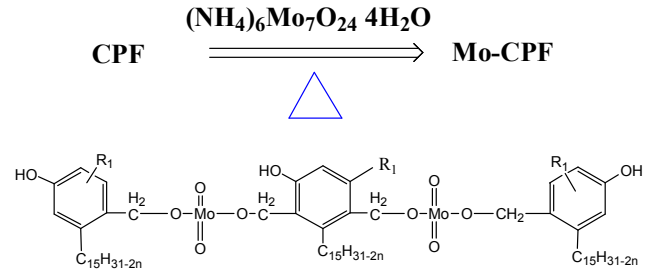

R_1=CH_2OH, -H

Scheme.2

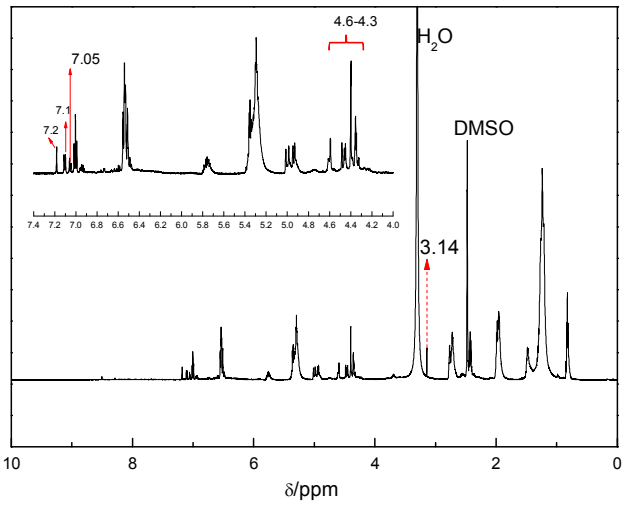

Fig.1

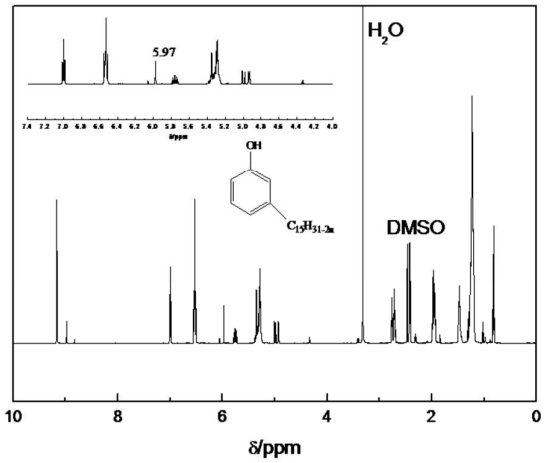

Fig.2

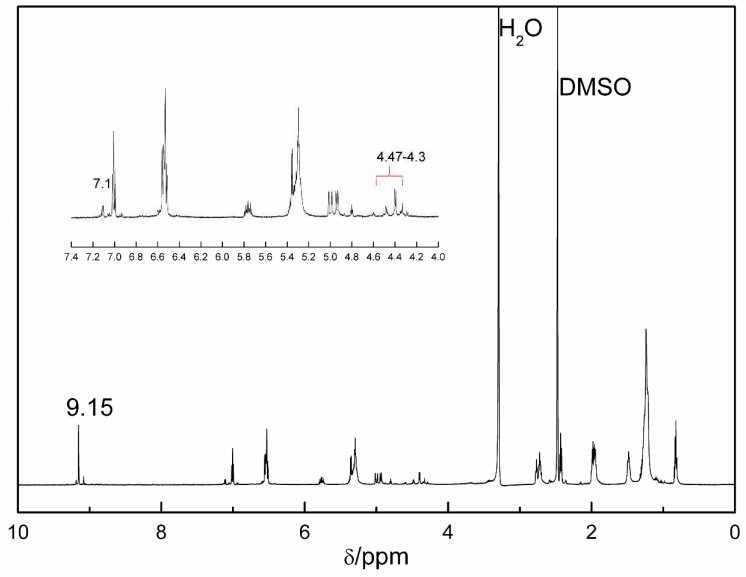

Fig.3

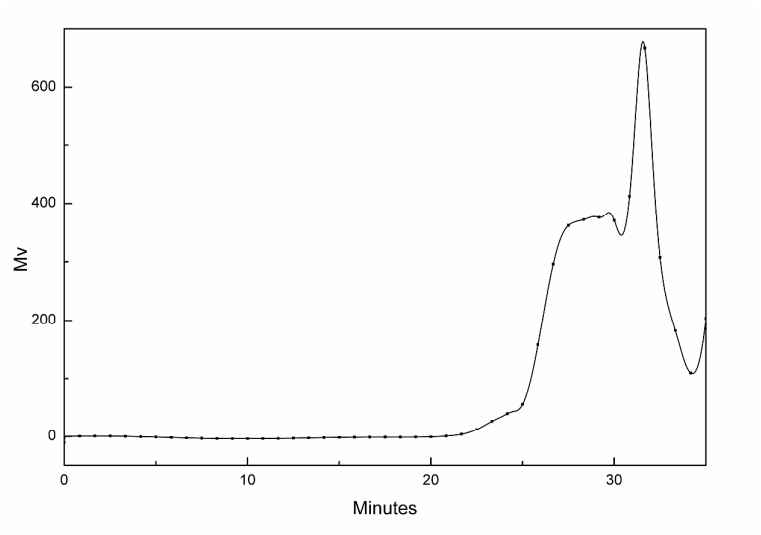

Fig.4

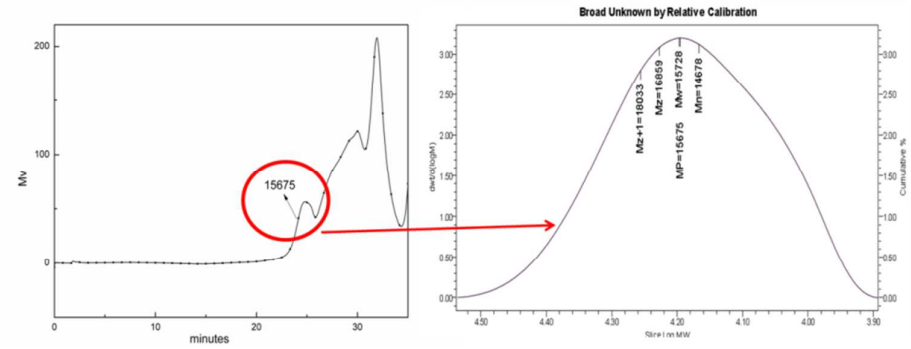

Fig.5

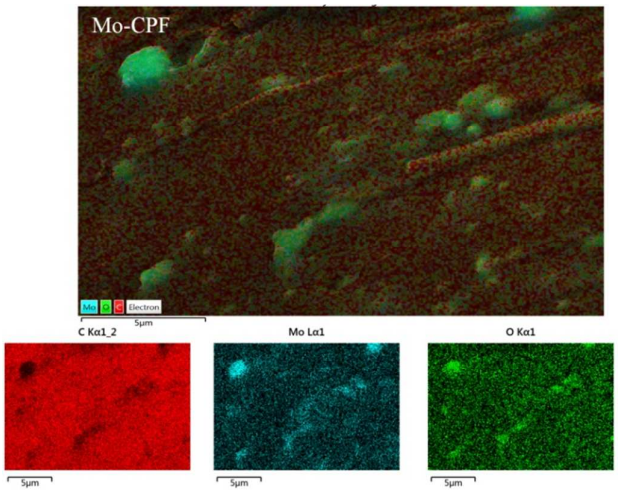

Fig. 6

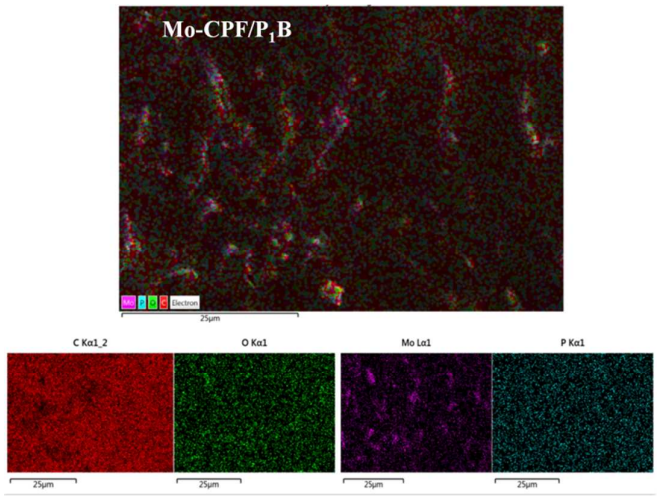

Fig. 7

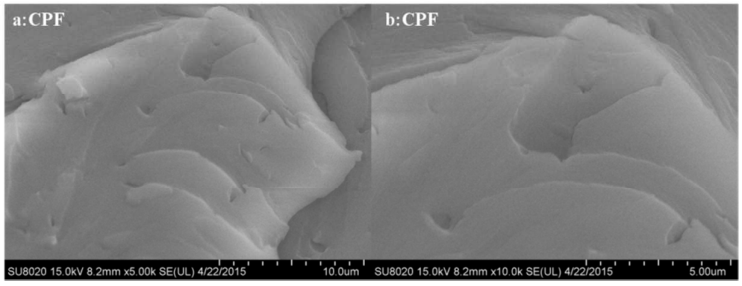

Fig.8

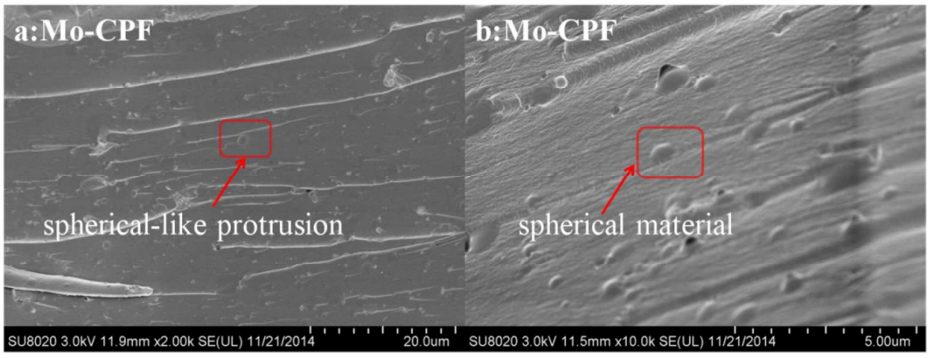

Fig. 9

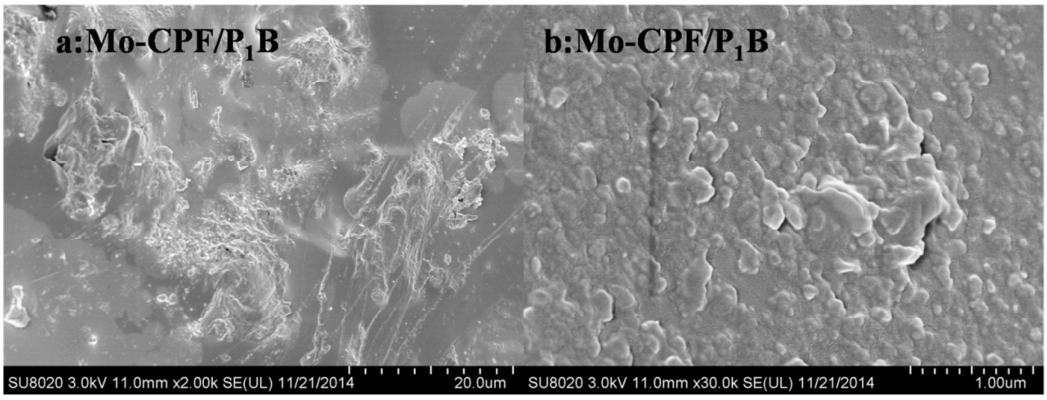

Fig. 10

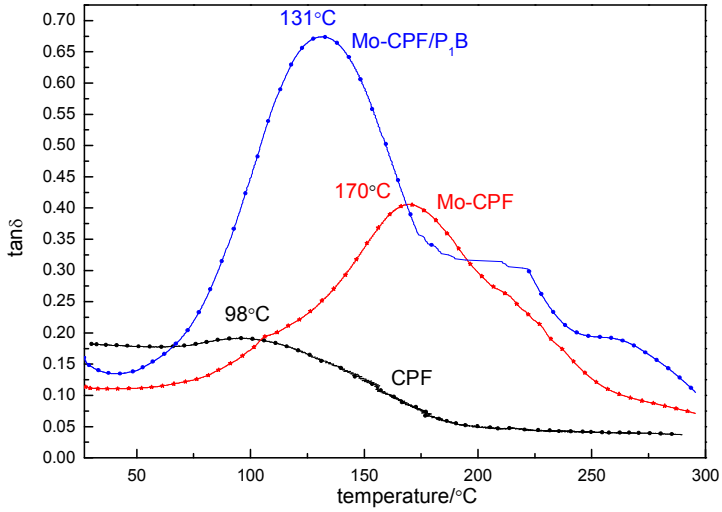

Fig. 11

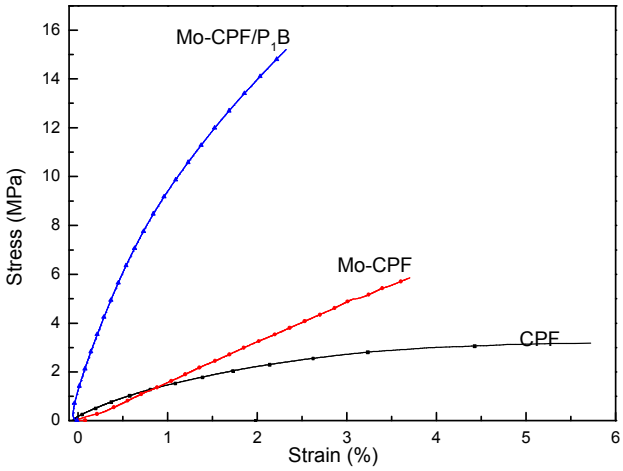

Fig.12

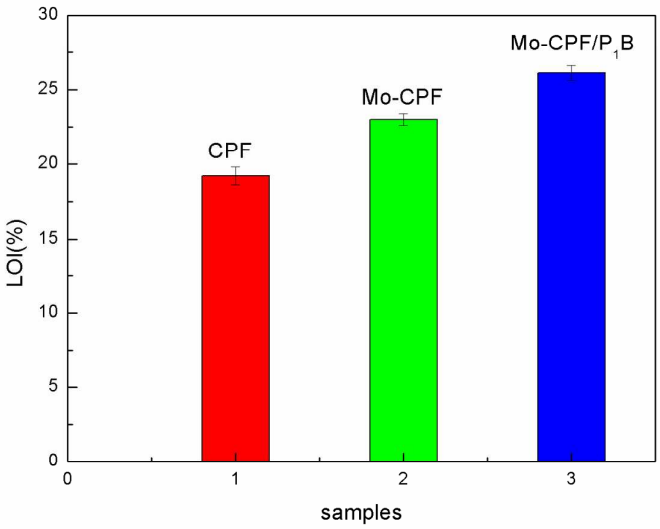

Fig.13

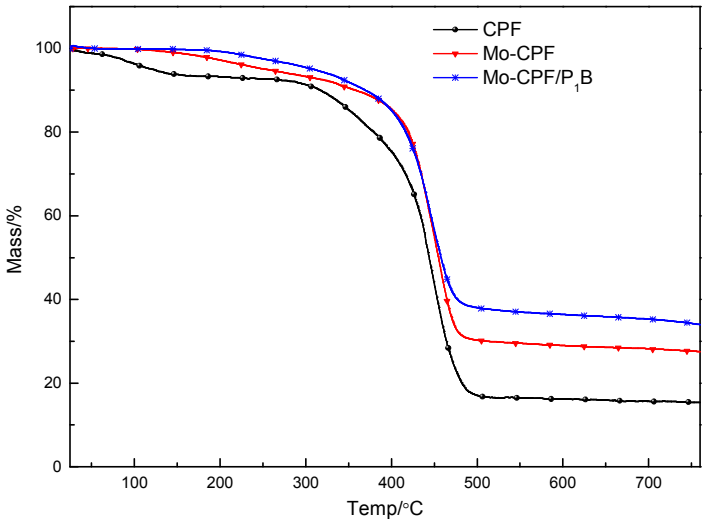

Fig.14

Fabrication and Property of Hybrid Mo-CPF/P_1B from cardanol

Guomei Xu [1, 2]·Tiejun Shi[1] ·Yu Xiang [1] ·Wei Yuan[1]·Quan Wang[1]

1 School of Chemistry and Chemical Engineering of Hefei University of Technology, Hefei, 230009, People's Republic of China

2. School o f Materials and Chemical Engineering of West Anhui University, Anhui, Lu'an, 237012, People's Republic of China

Table 1 Thermal property of CPF, Mo-CPF and Mo-CPF/P_1B

specimens	CPF	Mo-CPF	Mo-CPF/ P_1B
T_5(℃)	120	306	288
T_{10}(℃)	306	374	359
residues at 800℃ (%)	15	27	34
weight content of P (%)	0	0	1.78
weight content of Mo (%)	0	5.43	0.91
LOI(%)	19.2	23	26.1
Tg(℃)	98	170	131
flexural modulus(MPa)	123.7	167.7	1019

Table 2 Molecular weight and molecular weights distribution of Mo-CPF

Distribution Name	Mn/Daltons	Mw/Daltons	Polydispersity($\frac{Mw}{Mn}$)
	14678	15728	1.072

[1]Correspondence to: Tiejun Shi (stjhfut@163.com.)